A Multicomponent Crystal Approach with Increased Permeability of Cocrystal of Emtricitabine with Zwitterionic L-Proline

Daliya K. Shajan,[a] Palanisamy Kandhan,[b] Alexey N. Kuznetsov,[c] Vladimir V. Chernyshev[c,d*], Palash Sanphui*[,a]

[a]Department of Chemistry, Faculty of Engineering and Technology, SRM Institute of Science and Technology, Kattankulathur, Chennai, Tamil Nadu 603203, India. E-mail: palashi@srmist.edu.in

[b]Department of Chemistry, Center for Drug Discovery, Design, and Delivery (CD4), Southern Methodist University, Dallas, Texas 75275, United States.

[c]Department of Chemistry, M. V. Lomonosov Moscow State University, 1-3 Leninskie Gory, Moscow 119991, Russian Federation. E-mail: vladimir@struct.chem.msu.ru

[d]A. N. Frumkin Institute of Physical Chemistry and Electrochemistry RAS, 31 Leninsky Prospect, Moscow 119071, Russian Federation.

Table of contents

Figure S8. PXRD patterns of ECB, ECB BA and ECB PRL after diffusion study

Figure S9. PXRD pattern of ECB-PRO cocrystals after humidity exposure

Figure S10. PXRD pattern of ECB-PRL at 50^{o}C (1h)

Table S1. Summary of pharmaceutical cocrystals with proline (reported)

S.No	Cocrystals	Property Enhancment	BCS Class	Reference
1	Indomethacin and L-proline	Permeability and solubility	II	*New J. Chem.*, 2020,44, 3930-3939
2	Hydrochlorothiazide and L-proline	Permeability and solubility	IV	J. Pharm. Sci. 00 (2024) 1-12
3	Azetazolamide and L-proline	Permeability and solubility	IV	CrystEngComm, 2019, 00, 1-3
4	Naringenin and L-proline	Solubility and oral bioavailability	II	AAPS PharmSciTech (2019) 20:115
5	Fenofibric acid- L-proline	Solubility and dissolution	II	J Res Pharm 2024; 28(4): 974-981
6	Glicalazide and L-proline	Solubility and dissolution	II	Futur J Pharm Sci 7, 124 (2021).
7	Bezafibrate and L-proline	Solubility and dissolution	II	Available at SSRN: https://ssrn.com/abstract=4862669
8	Benzylthio acetic acid and L- proline	Structure analysis	-	*Molecules* 2022, *27*, 8203.
9	Itraconozole and L-prline	Dissolution	II	J. Drug Deliv. Sci. Technol 28 (2015) 46e55
10	Puerarin and L- proline	Solubility	IV	Int J Mol Sci . 2021 Jan 18;22(2):928.
11	Ezetimibe and L-proline	Dissolution	II	CrystEngComm, 2014, 16, 8984–8993
12	Lamotriginine and L-proline	Dissolution	II	Indones. J. Pharm, *34*(4), 574-583.
13	Sparfloxacin and L-proline	Dissolution	II	*Chem. Commun.,* 2016, 52, 12610--12613
14	Naproxen and L-prolinne	Structural aspects	II	CrystEngComm, 2014, 16, 8185–8196
15	Oxyreservetol and L-proline	Solubility and dissolution	IV	Int. J. Pharm *587 (2020) 119630*
16	Ipraglifozin and L-proline	Stability	II	Patent - KR102097250B1
17	Flavanoids and L-proline	dissolution	IV	Cryst. Growth Des. 2016, 16, 2348-2356
18	Benzoic acid L- proline	structure	-	Acta Cryst. (2017). E73, 369–371
19	Nebivilol Hydrochloride and L-	Dissolution	II	Int. J. Pharm. Res. *13*(5), 53–61

	proline			
20	Fumaric acid and L-proline	Structure analysis	-	Cryst. Growth Des, 13(6), 2373–2389
21	Curcumin and L-proline	Solubility and permeability	IV	. bioRxiv (Cold Spring Harbor Laboratory) 2023
22	**5-Flourouracil** and L-	Solubility and permeability	**III**	Int. J. Pharm. 2022, 617, 121635
23	Diclophenac and L-proline	Solubility and stability	II	Eur J Pharm Sci 2018, 117,168-176
24	Myricetin and L-proline	Dissolution	II	Eur J Pharm Biopharm, 107, 151–159
25	Ibuprofen and L-proline	Dissolution	II	J. Drug Deliv. Sci. Technol 67 (2022) 103003
26	Rutin and L-proline	Solubility and bioavailability	II	Cryst. Growth Des, 24(13), 5637–5647
27	Tocopherol and L-proline	Solidification and stabilization	II	Int. J. Pharm, *592*, 120057–120057.
28	**Pravastatin sodium** and L-proline	Bioavailability	**III**	Cryst. Growth Des. 2024, 24, 5309-5323

Table S2. Cocrystal screening of ECB with L-amino acids[a]

	Amino acids	**XRD**
1	Proline	New peaks
2	Aspartic acid	PM
3	Arginine	PM
4	Glutamine	PM
5	Lysine	PM
6	Histidine	PM
7	Threonine	PM
8	Serine	PM
9	Cysteine	PM
10	Glycine	PM
11	Leucine	PM
12	Isoleucine	PM
13	Phenylalanine	PM
14	Tyrosine	PM
15	Tryptophan	PM
16	Valine	PM
18	Metheonine	PM

[a]PM denotes physical mixture

Table S3. Atomic coordinates of ECB-PRL obtained in DFT-D optimization with the unit cell dimensions fixed to experimental values *a, b, c* = 5.1647, 25.1972, 12.3411 Å (Volume = 1606 Å^3).

Atom	*x*	*y*	*z*
C1	0.23081	-0.07773	0.22640
C2	0.12474	-0.01021	0.09509
C3	-0.11498	-0.01518	0.25751
C4	0.37810	-0.10308	-0.04402
C5	0.03533	-0.05956	0.29041
C6	0.66325	-0.15938	0.07233
C7	0.48251	-0.07261	0.05388
C8	0.71983	-0.19763	0.16478
F1	-0.02941	-0.08511	0.38332
H3	0.44654	-0.23920	0.22895
H3A	-0.39805	0.03764	0.29245
H3B	-0.37334	-0.01371	0.38858
H1	0.34866	-0.11224	0.24698
H4A	0.51849	-0.09988	-0.11056
H4B	0.19018	-0.08864	-0.07142
H6	0.82710	-0.16315	0.01201
H7	0.58335	-0.03624	0.02784
H8A	0.76659	-0.23634	0.12800
H8B	0.89770	-0.18353	0.20659
N1	0.27249	-0.05441	0.12838
N2	-0.05523	0.00990	0.16433
N3	-0.31501	0.00260	0.31675
O1	0.16748	0.00892	0.00330
O2	0.65399	-0.10550	0.11214
O3	0.51309	-0.20251	0.24033
S1	0.35307	-0.17083	0.00401
C9	-0.07332	0.17038	0.20379
C10	-0.09583	0.21220	0.11344
C11	-0.11945	0.17775	0.01186
C12	0.08925	0.13708	0.03068
C13	-0.33998	0.15550	0.25146
H4C	-0.04774	0.08868	0.15823
H4D	0.24198	0.11615	0.18540
H9	0.05189	0.18421	0.27071
H10A	-0.25948	0.23886	0.12701
H10B	0.08134	0.23632	0.11083
H11A	-0.09483	0.19852	-0.06568
H11B	-0.31491	0.15805	0.01018
H12A	0.08072	0.10018	-0.01606
H12B	0.28618	0.15509	0.01884

N4	0.06077	0.12391	0.14966
O4	-0.42558	0.10844	0.24182
O5	-0.45578	0.19336	0.29734

Table S4. Atomic coordinates of ECB-PRL obtained in DFT-D optimization without any constraints, which led to the unit cell dimensions *a, b, c* = 4.4714, 25.3756, 12.1724 Å (Volume = 1381 Å^3).

Atom	*x*	*y*	*z*
C1	0.25109	-0.07722	0.22981
C2	0.15921	-0.00681	0.10187
C3	-0.13758	-0.01323	0.26073
C4	0.37672	-0.10246	-0.04258
C5	0.02606	-0.05815	0.29329
C6	0.71870	-0.16169	0.06736
C7	0.53159	-0.07440	0.05288
C8	0.76834	-0.20026	0.16055
F1	-0.07706	-0.08594	0.38036
H3	0.44084	-0.23534	0.23112
H3A	-0.46179	0.03893	0.29871
H3B	-0.43772	-0.01331	0.39255
H1	0.37365	-0.11330	0.24890
H4A	0.50403	-0.09693	-0.11838
H4B	0.14995	-0.08828	-0.05375
H6	0.90953	-0.16711	0.00672
H7	0.65823	-0.04010	0.02290
H8A	0.79230	-0.23953	0.12316
H8B	0.98780	-0.19110	0.20171
N1	0.31290	-0.05298	0.13308
N2	-0.05371	0.01297	0.16916
N3	-0.37078	0.00353	0.32016
O1	0.23308	0.01408	0.01285
O2	0.72254	-0.10903	0.10924
O3	0.52912	-0.19943	0.23728
S1	0.36605	-0.17095	-0.00118
C9	-0.04044	0.17420	0.19232
C10	-0.10230	0.21277	0.09774
C11	-0.14309	0.17537	0.00053
C12	0.09735	0.13682	0.01777
C13	-0.32033	0.16015	0.25317
H4C	-0.06012	0.09334	0.15431
H4D	0.29056	0.11534	0.17323
H9	0.13243	0.18886	0.25138
H10A	-0.29641	0.23700	0.11597
H10B	0.08881	0.23861	0.08435

H11A	-0.13918	0.19276	-0.08195
H11B	-0.36909	0.15458	0.00858
H12A	0.09504	0.09996	-0.02851
H12B	0.32296	0.15678	0.00264
N4	0.08303	0.12534	0.13828
O4	-0.40346	0.11198	0.25544
O5	-0.45783	0.19795	0.29704

Table S5. The calculated BEs of different conformations of ECB-PRL dimer.

Complex	BE (kcal/mol)
ECB-PRL 1	-30.05
ECB-PRL 2	-20.73
ECB-PRL 3	-34.01
ECB-PRL 4	-21.63
ECB-PRL 5	-18.76
ECB-PRL 6	-46.40
ECB-PRL 7	-18.00
ECB-PRL 8	-17.00
ECB-PRL 9	-13.46
ECB-PRL 10	-11.01
ECB-PRL 11	-12.33
ECB-PRL 12	-8.46
ECB-PRL 13	-9.45
ECB-PRL 14	-12.33
ECB-PRL 15	-10.34
ECB-PRL 16	-9.85

Table S6. Hydrogen bonding geometry of ECB-PRL cocrystal

	D–H···A	**D-H/ Å**	**H···A/Å**	**D···A/Å**	**D-H···A/°**
ECB-PRL	O3−H3···O5	0.83	2.03	2.799(7)	155
	N3−H3A···O4	0.86	2.24	3.045 (9)	155
	N3−H3B···O1	0.86	2.21	2.873(10)	133
	N4−H4C···N2	0.90	2.22	2.999(9)	145
	N4−H4D···O4	0.90	1.96	2.847(12)	168

Table S7. Calculation of octanol-water partition coefficients of ECB and cocrystal

Solid forms	C_w (mg/mL)	C_0 (mg/mL)	C_E (mg/mL)	Log (C_0/Cw)	Log ($C_{initial}$-C_E)/C_E
ECB	0.5321	0.08552	0.4450	-0.7940	-0.7162
ECB-BA	0.3832	0.06556	0.3201	-0.7666	-0.6886
ECB-PRL	0.92667	0.2039	0.7224	-0.6574	-0.5959

Table S8. Percentage contribution of polar and non-polar contacts

Inter molecular contacts	**ECB**	**ECB-PRL**	**ECB-BA**
C-C	0.5	0	6.4
H-H	25.9	42.5	36.6
C-H	7.1	5.0	5.3
Total non-polar contacts (%)	**33.5**	**47.5**	**48.3**
Polar contacts			
O-H	22.2	22.5	26.1
N-H	4.7	4.4	6.5
H-F	8.3	9.4	7.4
O-F	2.3	1.6	1.7
S-H	13.8	8.5	2.7
C-O	0.6	3.9	0.9
Total polar contacts (%)	**51.9**	**50.3**	**45.3**

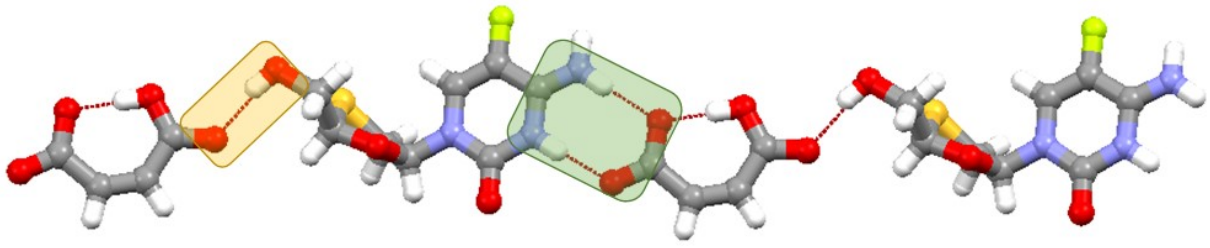

(a)

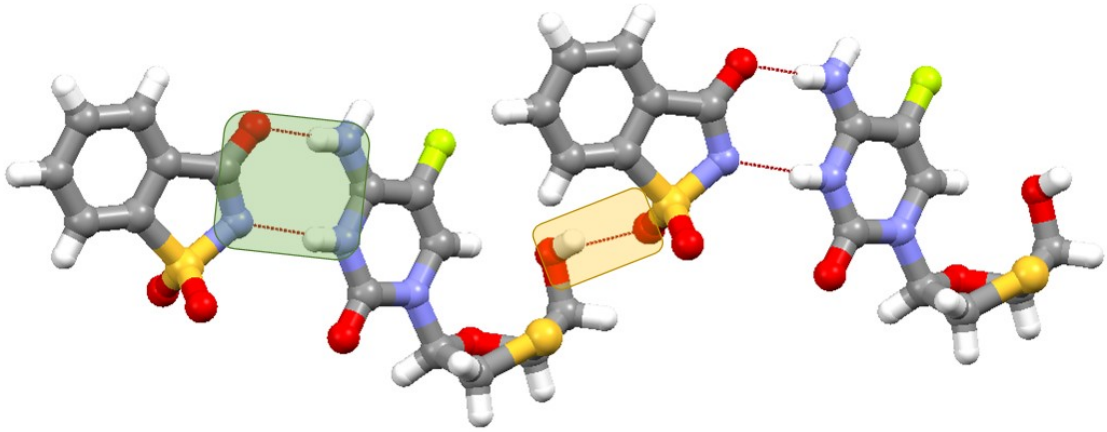

(b)

Figure S1. Alternate hydrogen bonding pattern of a) ECB-maleate and b) ECB-saccharinate salts that form 1 D chain motif.

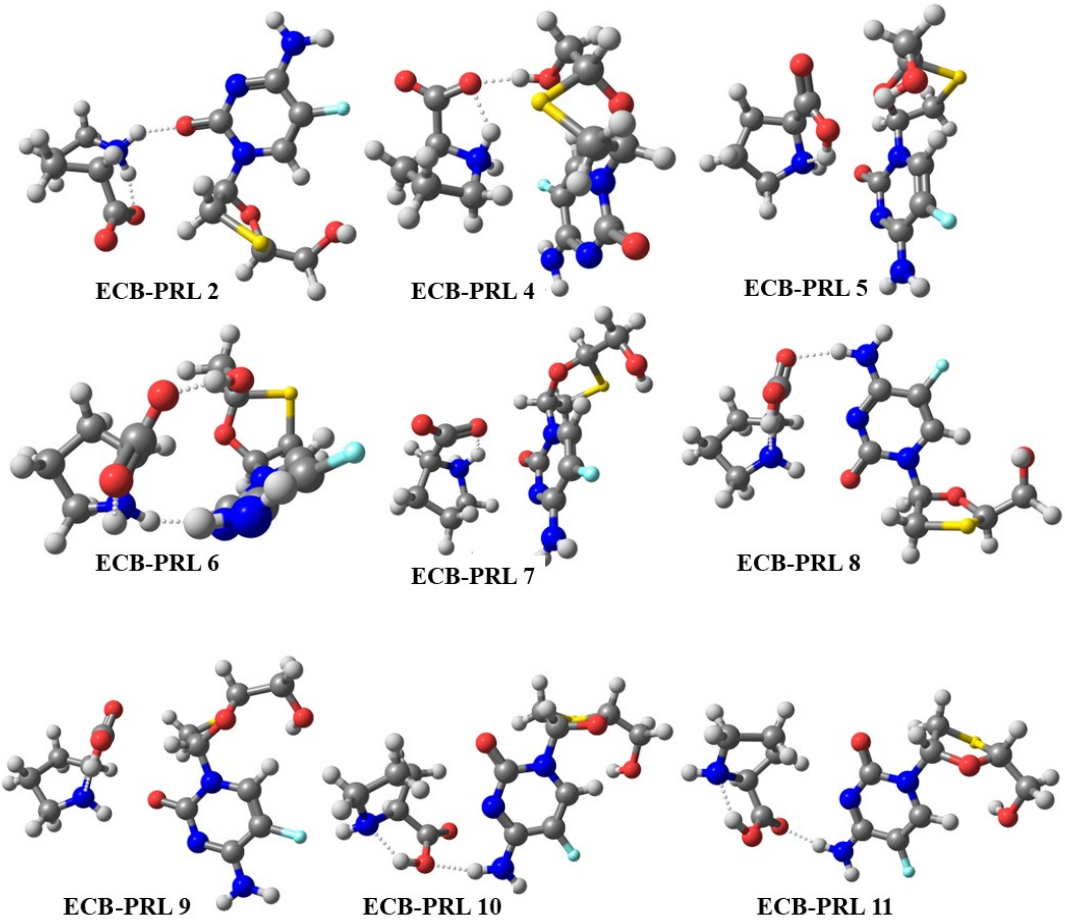

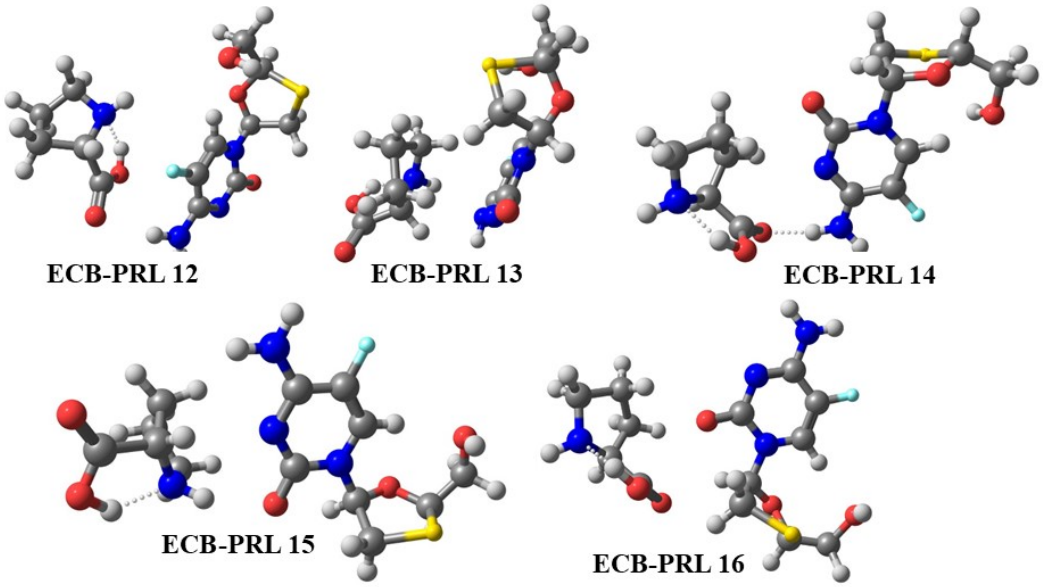

Figure S2. All the optimized geometries of ECB-PRL with different conformations.

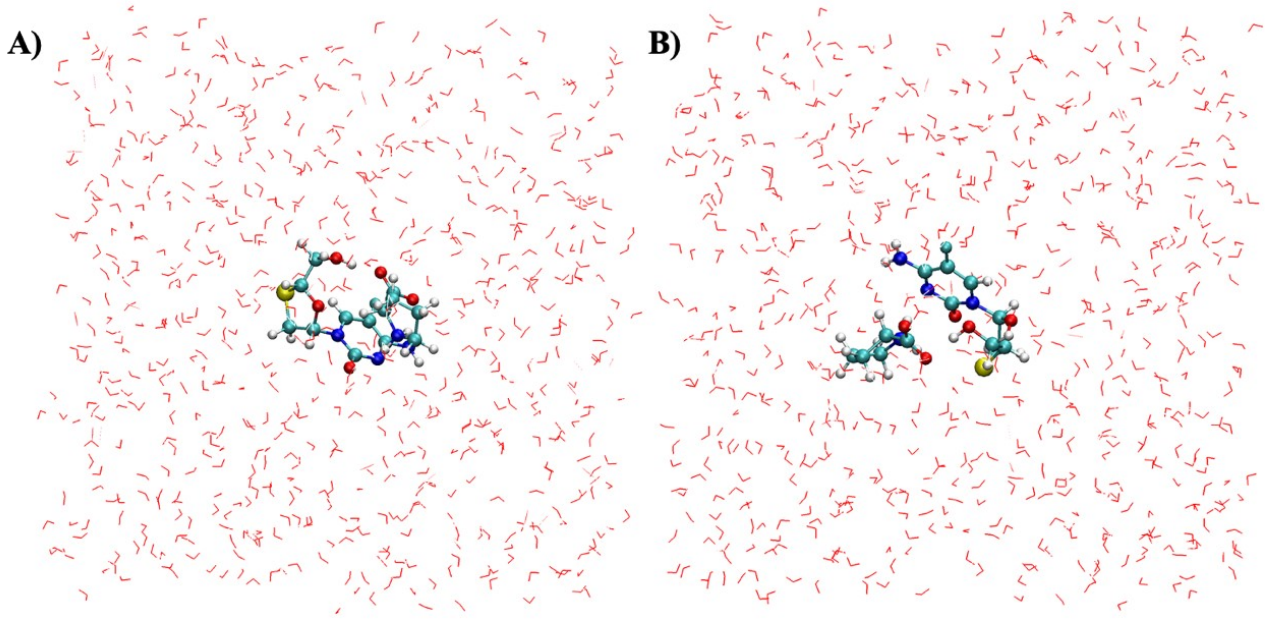

Figure S3. The initial conformations taken for MD simulations.

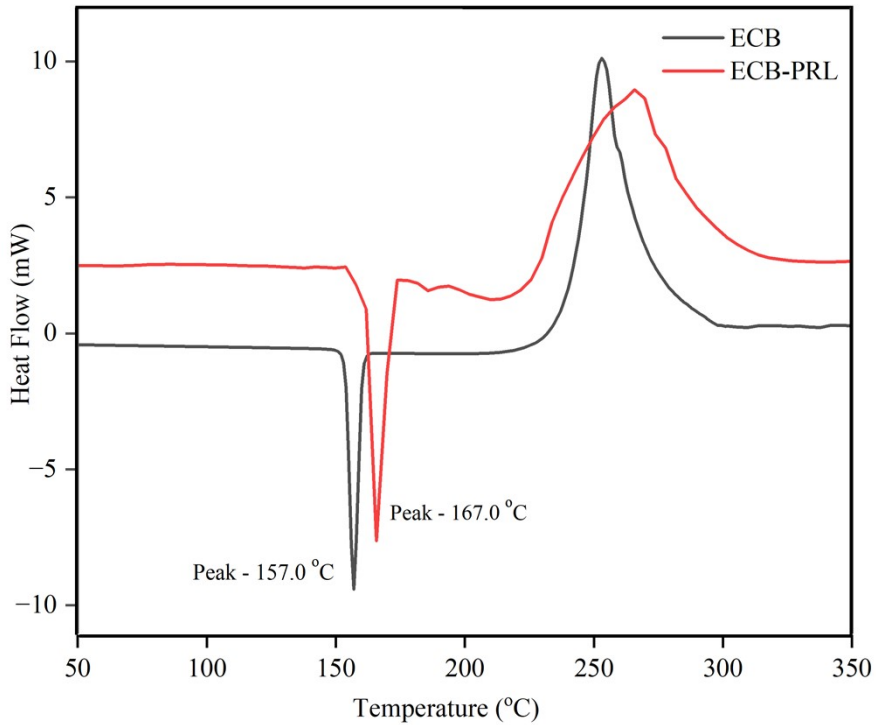

Figure S4. Combined DSC-TGA of ECB-PRL

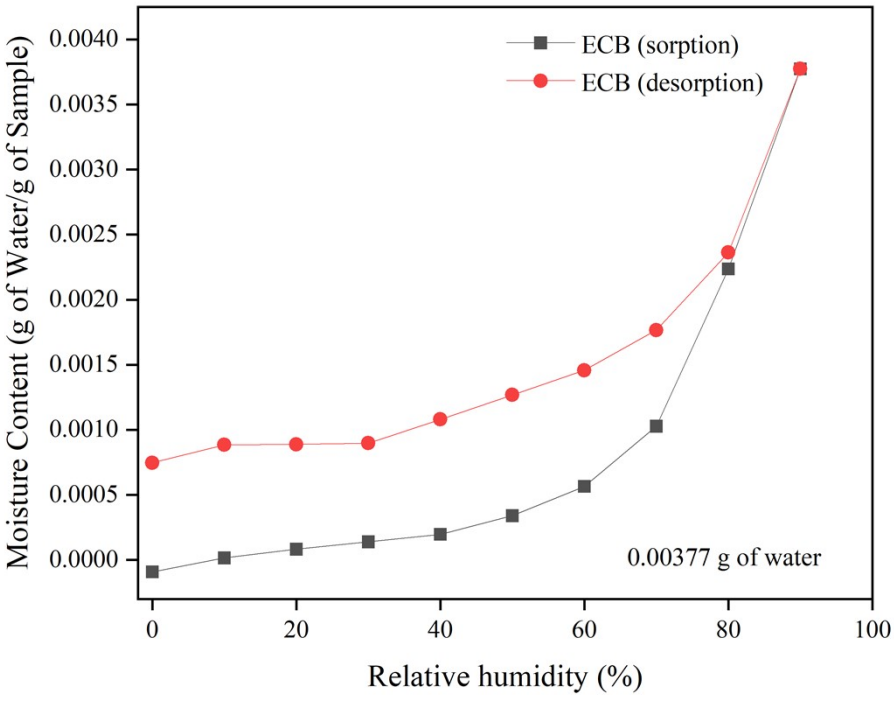

(a)

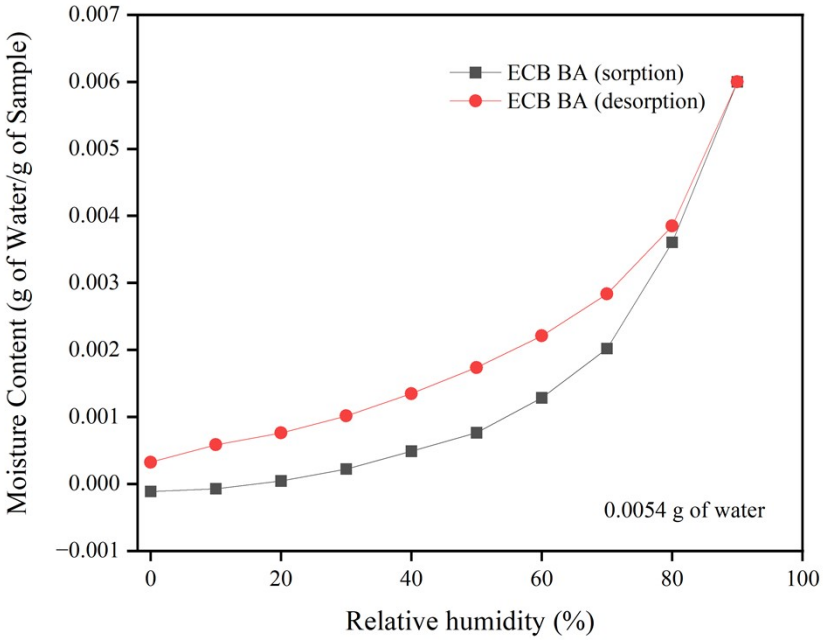

(b)

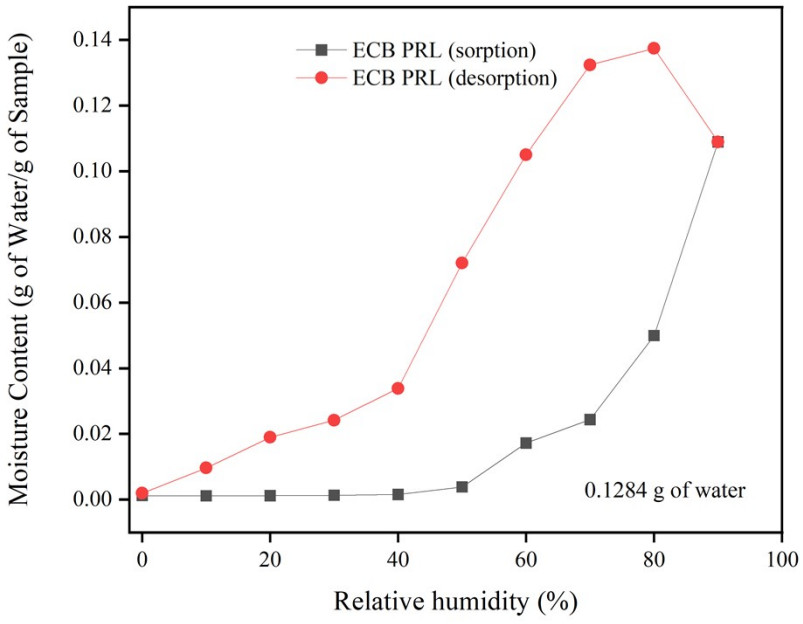

(c)

Figure S5. Sorption-desorption cycles of a) ECB and b, c) cocrystals

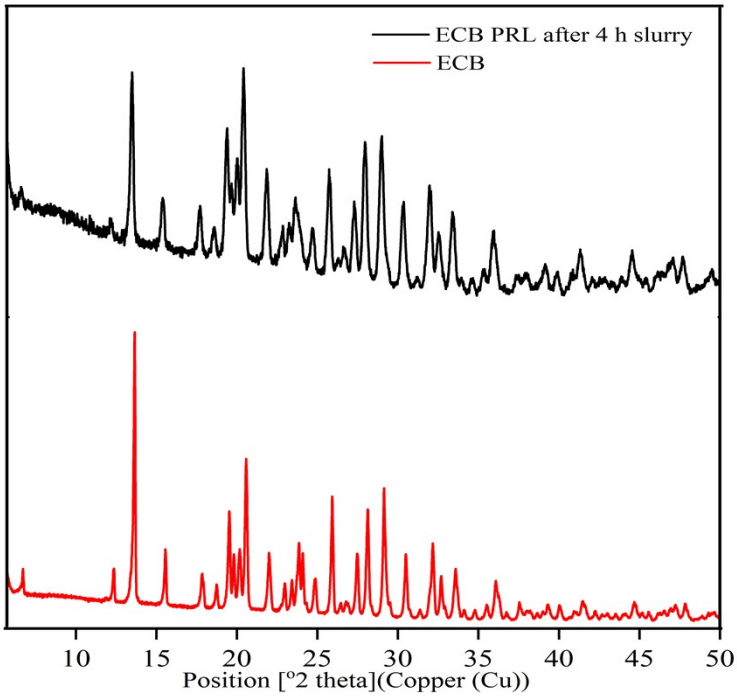

Figure S6. PXRD pattern of ECB-PRL after 4 h solubility experiment was transformed to native drug

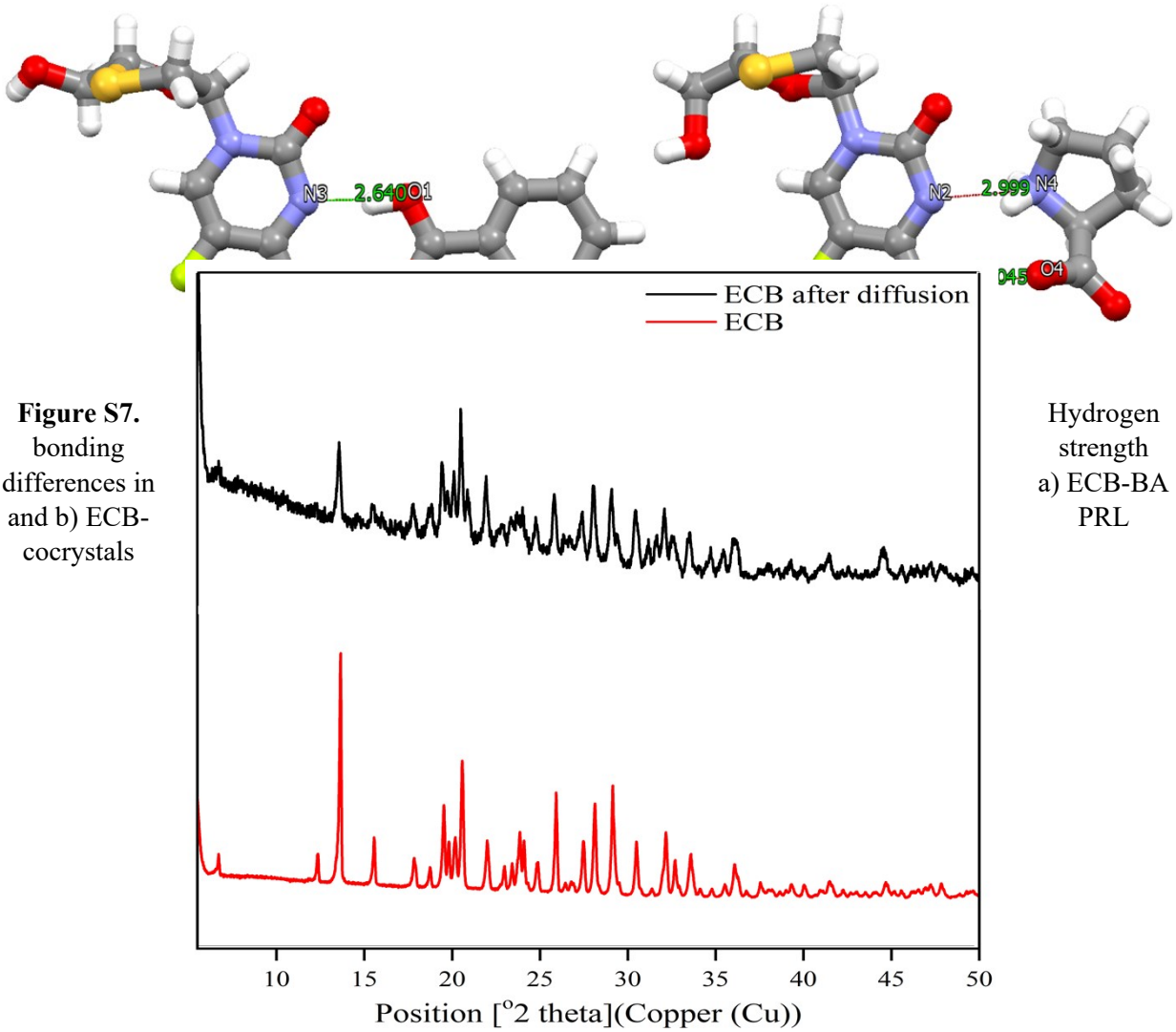

Figure S7. Hydrogen bonding differences in a) ECB-BA and b) ECB-PRL cocrystals

a)

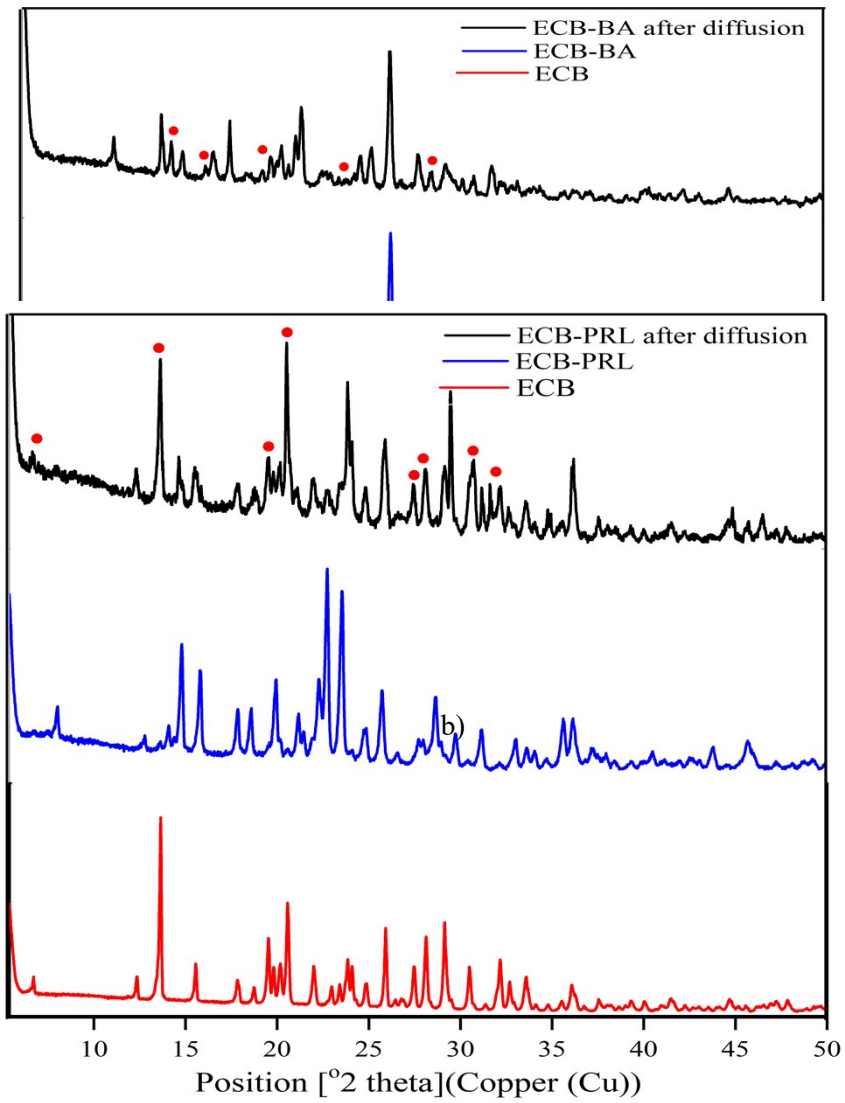
ECB-BA after diffusion
ECB-BA
ECB
ECB-PRL after diffusion
ECB-PRL
ECB
10
15
20
25
30
35
40
45
50
Position [°2 theta](Copper (Cu))

b)

c)

Figure S8. PXRD of a) ECB, and b,c) its cocrystals after diffusion study (the red spots correspond to the ECB peak)

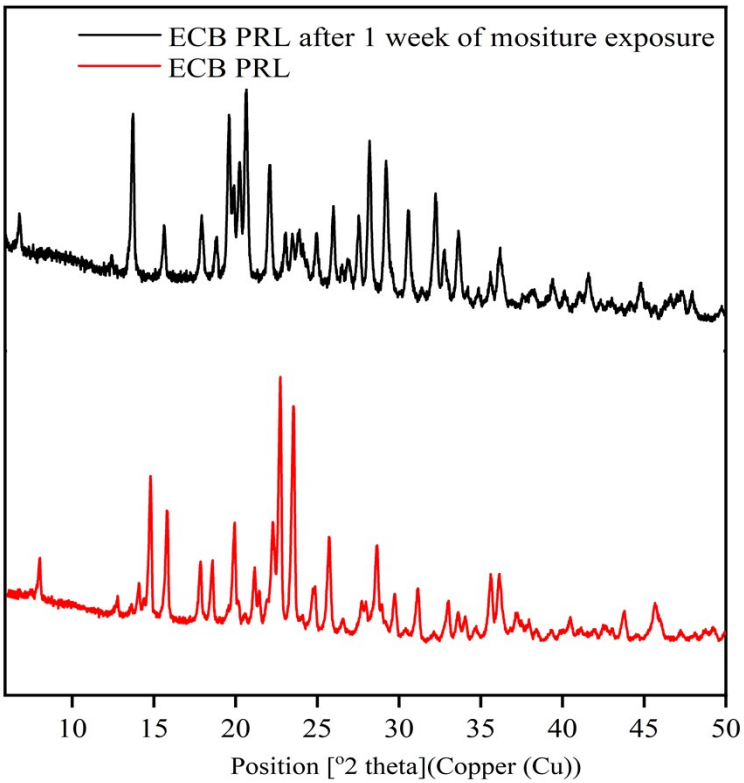

Figure S9. PXRD pattern after moisture exposure

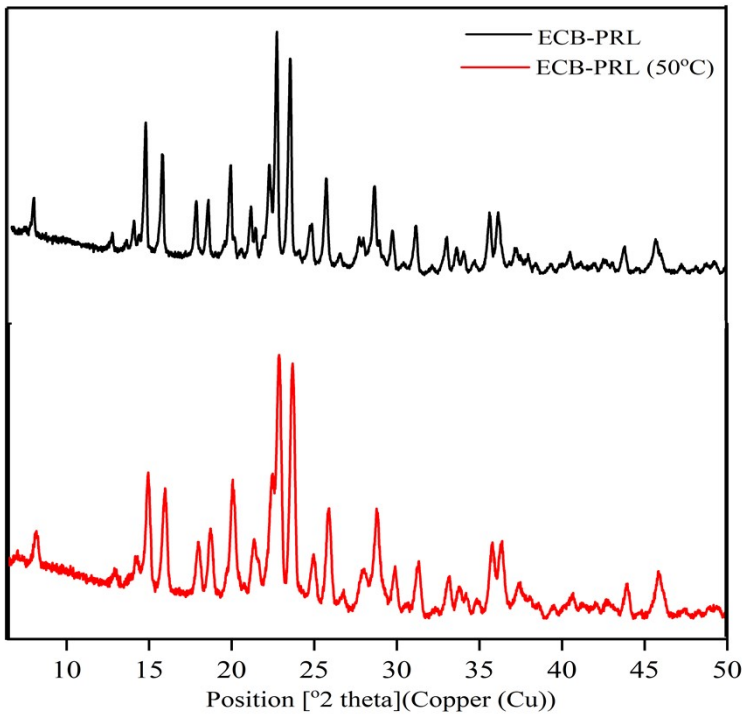

Figure S10. PXRD pattern of ECB-PRL cocrystal at 50°C confirmed its thermal stability.